*International Journal of Thermophysics, Vol. 15, No. 6, 1994*

# Simulation of Bead-and-Spring Chain Models for Semidilute Polymer Solutions in Shear Flow[1]

**S. W. Fetsko[2] and P. T. Cummings[3,5]**

We report preliminary results of simulations of the steady-state rheological behavior for semidilute polymer solutions of bead-and-spring chain models in planar Couette flow. The simulations include examination of the effects of excluded volume, hydrodynamic interactions, and density. Hydrodynamic interactions are modeled by the Rotne–Prager–Yamakawa tensor. The simulations are based on the nonequilibrium Brownian dynamics algorithm of Ermak and McCammon. In addition to the spring potential between neighboring beads in the chain, the interaction between any two beads in the solution is modeled using a shifted, repulsive Lennard–Jones potential. Lees–Edward sliding brick boundary conditions are used for consistency with the Couette flow field.

**KEY WORDS:** Brownian dynamics; rheology; semidilute polymer solutions; viscosity.

## 1. INTRODUCTION

Many studies of the dynamics of polymeric liquids have focused primarily on the infinitely dilute and melt regimes [1, 2]. In contrast, few studies have explored the concentration regimes between these two extremes. Of interest in this paper is the semidilute region, where the polymer chains

[1] Paper presented at the Twelfth Symposium on Thermophysical Properties, June 19–24, 1994, Boulder, Colorado, U.S.A.

[2] Department of Chemical Engineering, University of Virginia, Charlottesville, Virginia 22903-2442, U.S.A.

[3] Department of Chemical Engineering, University of Tennessee, Knoxville, Tennessee 37996-2200, U.S.A.

[4] Chemical Technology Division, Oak Ridge National Laboratory, Oak Ridge, Tennessee 37831-6268, U.S.A.

[5] To whom correspondence should be addressed.



0195-928X/94/1100-1085$07.00/0 

interact with one another, but the density is low enough that entanglements between the chains are considered negligible.

The purpose of this study is to model the behavior of semidilute polymer solutions using nonequilibrium Brownian dynamics (NEBD). NEBD has been shown to model effectively the behavior of bead-and-spring chains at infinite dilution in both planar Couette and elongational flow [3–6]. At the finite dilutions reported in this paper, NEBD simulations of bead-and-spring models for polymer solutions are performed with interactions between bonded beads modeled by the finitely extensible nonlinear elastic (FENE) potential (see below), with the interactions between all beads (bonded and non-bonded) modeled by a shifted, repulsive Lennard–Jones potential (see below), and with Lees–Edward sliding brick boundary conditions applied to the finite-sized simulation cell [7]. By means of this technique, the effects of excluded volume (EV), hydrodynamic interactions (HI), and density on the rheological properties can be studied.

Prior modeling of the interactions between beads in a semidilute polymer solution by means of a repulsive potential has been reported by Hess [8] and Ng and Leal [9] in their interacting dumbbell model. With this model they were able to predict shear-thinning of both the viscosity and the first normal stress coefficient, in agreement with experimental observations on semidilute polymer solutions [10].

Bead-and-spring models have also been used in studies of the rheological properties of melts. Grest and Kremer [11, 12] used a molecular dynamics approach, where each monomer was weakly coupled to a frictional background and a heat bath, to study melt behavior, including the crossover from Rouse to reptation dynamics. Bitsanis and Hadziannou [3] used molecular dynamics to study the structure and dynamics of confined polymer melts. Rudisill and Cummings [14] used nonequilibrium molecular dynamics (NEMD) to calculate the rheological properties of melts of rigid and FENE dumbbells with Lennard–Jones interactions between beads in different molecules. Dlugogorski et al. [15, 16] have also performed NEMD simulations of FENE dumbbells with Lennard-Jones interactions.

Our simulation algorithm, as described in Section 2, enables us to study the rheological behavior in the concentration range between infinite dilution and melts. The results from the simulation study are presented in Section 3 and their significance is discussed in Section 4.

## 2. METHODS

We employ the position Langevin level BD simulation algorithm of Ermak and McCammon [17] as modified by Diaz et al. [18] to include

the effects of a solvent flow field. The major details of the simulation algorithm have been described in previous papers [3–5]. The key assumptions of this algorithm are that the solvent is Newtonian, the solvent is configurationally and kinetically equilibrated on the time scale of the solvent motion, and the peculiar (nonstreaming) velocity of the solute molecules is at kinetic equilibrium (Maxwell–Boltzmann distribution) due to frequent collisions with solvent molecules. The additions required to model semidilute polymer solutions are presented here.

The first addition required is to model the repulsive interactions between any two beads in the solution. As mentioned previously, this is done by means of a shifted, truncated Lennard–Jones potential. The potential and force law are

$$u_{LJ}(r) = 4\varepsilon\left[\left(\frac{\sigma_{LJ}}{r}\right)^{12} - \left(\frac{\sigma_{LJ}}{r}\right)^{6} + \frac{1}{4}\right], \qquad r \leqslant 2^{1/6}\sigma_{LJ} \tag{1}$$

$$u_{LJ}(r) = 0, \qquad r > 2^{1/6}\sigma_{LJ} \tag{2}$$

and

$$\vec{F}_{LJ}(\vec{r}) - \frac{24\varepsilon}{\sigma_{LJ}}\left[2\left(\frac{\sigma_{LJ}}{r}\right)^{14} - \left(\frac{\sigma_{LJ}}{r}\right)^{8}\right]\frac{\vec{r}}{\sigma_{LJ}}, \qquad r \leqslant 2^{1/6}\sigma_{LJ} \tag{3}$$

where $u_{LJ}(r)$ is the potential, $\vec{r}$ is the vector between the centers of the adjacent beads, $r = |\vec{r}|$, $\vec{F}_{LJ}(\vec{r})$ is the force, $\varepsilon$ is the Lennard–Jones energy parameter, and $\sigma_{LJ}$ is the Lennard–Jones length parameter. The interaction between neighboring beads in a molecule is given by the FENE potential

$$u_{FENE}(Q) = -\tfrac{1}{2} H Q_0^2 \ln(1 - Q^2/Q_0^2), \qquad Q < Q_0 \tag{4}$$

$$u_{FENE}(Q) = \infty, \qquad Q > Q_0 \tag{5}$$

and force law

$$\vec{F}(\vec{Q}) = -\frac{H\vec{Q}}{1 - Q^2/Q_0^2}, \qquad Q < Q_0 \tag{6}$$

where $\vec{Q}$ is the vector joining the centers of the two beads, $Q = |\vec{Q}|$, and $Q_0$ is the maximum extension of the bond. The FENE potential reduces to the Hookean spring potentials as $Q \to 0$ with spring constant $H$.

The Lees–Edward sliding-brick version of periodic boundary conditions [7] is used to replicate the central simulation cell infinitely in the $x$, $y$, and $z$ directions. The simulation cells above and below the central simulation cell in the $y$ direction are moved with a velocity that is determined by $\dot{\gamma}$, the shear rate. The minimum-image convention is used to

calculate the forces and diffusion tensor based on the closest image to the chosen bead. Periodic imaging is used to place a polymer chain back in the central simulation cell if its center of mass leaves the cell.

With these modifications, the rheological properties can be calculated using Kramers' expression for the stress tensor [1, 19], which is

$$\tau = -\eta_s \dot{\gamma} - n\langle \mathbf{RF} \rangle + nk_B T\mathbf{I} \tag{7}$$

where $\eta_s$ is the solvent viscosity, $\dot{\gamma}$ is the rate of strain tensor, which for shear flow has all components zeros except $\dot{\gamma}_{xy} = \dot{\gamma}_{yx} \equiv -\dot{\gamma}$, $n$ is the number density of chains, $k_B$ is Boltzmann's constant, $T$ is the absolute temperature, $\mathbf{I}$ is the unit tensor, and $\langle \ldots \rangle$ denotes an ensemble average, given by

$$\langle \mathbf{RF} \rangle = \frac{\sum_{\text{timesteps}} \sum_{\text{chains}} \sum_{1 \le i < j \le N_b} \mathbf{R}_{ij}\mathbf{F}_{ij}}{\sum_{\text{timesteps}}}$$

The shear viscosity may be expressed in terms of the stress tensor as

$$\eta \equiv -\tau_{xy}/\dot{\gamma} = \eta_s + n\langle R_x F_y \rangle/\dot{\gamma} \tag{8}$$

The dimensionless viscosity is defined as

$$\frac{\eta - \eta_s}{nk_B T\lambda_H} = \frac{\langle R_x F_y \rangle}{k_B T\lambda_H \dot{\gamma}} \tag{9}$$

where $\lambda_H = \zeta/4H$ is a characteristic time and $\zeta$ is the translational friction. From the stress tensor, the first normal stress coefficient

$$\Psi_1 = \frac{n[\langle R_x F_x \rangle - \langle R_y F_y \rangle]}{\dot{\gamma}^2} \tag{10}$$

can be calculated. The dimensionless first normal stress coefficient is given by

$$\frac{\Psi_1}{2nk_B T\lambda_H^2} = \frac{\langle R_x F_x \rangle - \langle B_y F_y \rangle}{2k_B T\lambda_H^2 \dot{\gamma}^2} \tag{11}$$

The results in this paper are given in terms of the dimensionless viscosity and first normal stress coefficient.

## 3. RESULTS

In this preliminary report of our work, we focus exclusively on a solution of FENE dumbbells. The parameters for the FENE dumbbells are

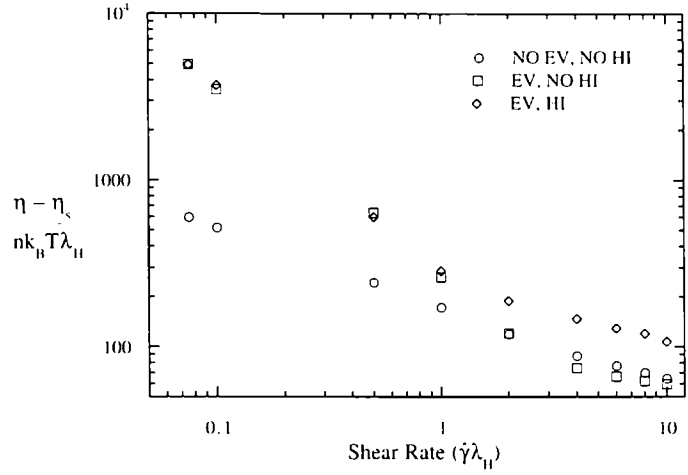


**Fig. 1.** Shear rate dependence of the viscosity for FENE dumbbells with $h = 67.5$.

those used by Grest and Kremer [11] to minimize the possibility of bond crossings. The parameters describing the simulation conditions are given in reduced units: All lengths are given in units of the bead diameter $\sigma$, masses in units of the bead mass $m$, and energies in units of $k_B T$. In these units, the spring constant is given by $H = 30$, the Lennard–Jones diameter by

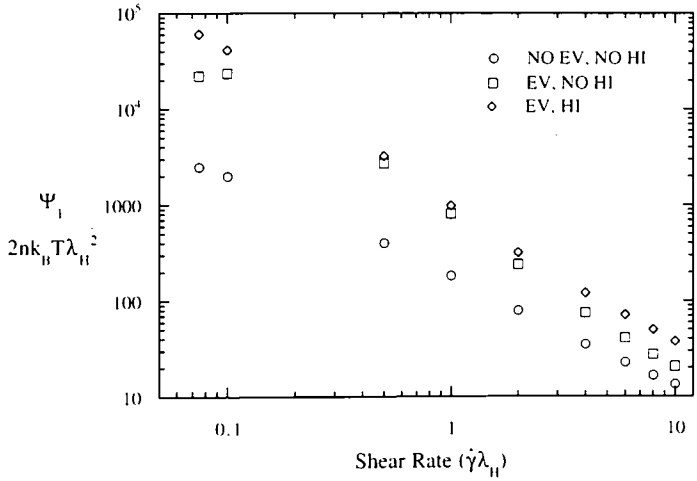


**Fig. 2.** Shear rate dependence of the first normal stress coefficient for FENE dumbbells with $h = 67.5$.

$\sigma_{LJ} = 1$, the Lennard–Jones energy by $\varepsilon = 1$, and the maximum spring extension by $Q_0 = 1.5$. The resulting FENE parameter is $b_{FENE} = HQ_0^2/k_B T = 67.5$.

Figure 1 shows the viscosity as a function of shear rate for the cases where EV and HI are not included, when EV but not HI is included, and when EV and HI are included. Figure 2 shows the first normal stress coefficient as a function of shear rate for the same three cases. All these results are for dumbbells at a dimensionless density of 0.01. The results at other densities are qualitatively similar. For all three cases, shear thinning behavior is observed in both the viscosity and the first normal stress coefficient. At low shear rates, the case where EV and HI are not included produces the lowest values for the viscosity and first normal stress coefficient. When EV is added, the range of bead–bead separations possible for bonded beads is reduced and the rheological properties increase. The inclusion of HI does not significantly affect the rheological properties at low shear rates since the reduction in drag caused by the hydrodynamic effect is minimal for dumbbells. We expect that it will be more significant for longer chains. At high shear rates, however, extra hydrodynamic drag is produced and the result is an increase in the viscosity and firts normal stress cofficient when HI is added [20–22].

Figure 3 shows the viscosity as a function of density for three different shear rates. The results are for the case where EV and HI are not included. For comparison the density of an infinitely dilute ($\rho^* = 0$) solution of dumbbells is also shown. At the lower densities, the viscosities are relatively insensitive to density, while at the higher densities the viscosity exhibits stronger density dependence, increasing with density as expected.

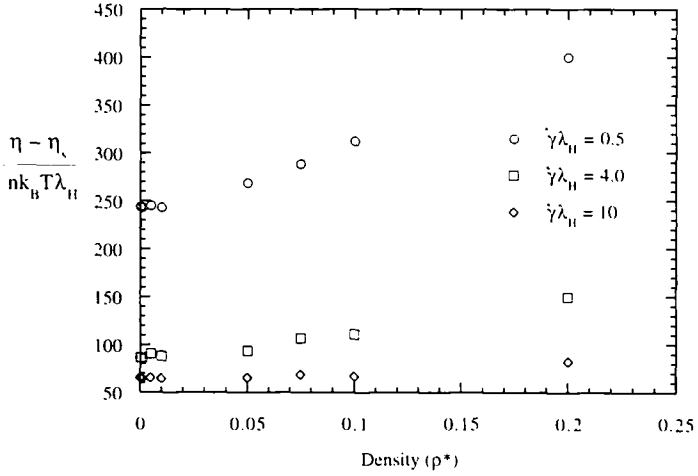


**Fig. 3.** Density dependence of the viscosity for FENE dumbbells with $b = 67.5$.

## 4. CONCLUSIONS

Preliminary results of Brownian dynamics simulations for semidilute polymer solutions of bead and spring chains undergoing shear flow have been presented. The effects of excluded volume, hydrodynamic interactions, and density have been studied. The predicted results are in qualitative agreement with experimental observations. Further study of the effect of chain length and of the time-dependent behavior is being performed.

## ACKNOWLEDGMENT

The authors gratefully acknowledge the support of this research by the National Science Foundation through Grant CTS-910136.

## REFERENCES

1. R. B. Bird, R. C. Armstrong, and O. Hassager, *Dynamics of Polymeric Liquids: Fluid Mechanics, Vol. 1*, 2nd ed. (Wiley, New York, 1987).
2. R. B. Bird, C. F. Curtiss, R. C. Armstrong, and O. Hassager, *Dynamics of Polymeric Liquids: Kinetic Theory, Vol. 2*, 2nd ed. (Wiley, New York, 1987).
3. J. W. Rudisill and P. T. Cummings, *J. Non-Newt. Fluid Mech.* **41**:275 (1991).
4. J. W. Rudisill, S. W. Fetsko, and P. T. Cumings, *Comp. Polym. Sci.* **3**:23 (1993).
5. S. W. Fetsko and P. T. Cummings, submitted for publication (1994).
6. B. H. A. A. van den Brule, *J. Non-Newt. Fluid Mech.* **47**:357 (1993).
7. A. W. Lees and S. F. Edwards, *J. Phys. C Solid State* **5**:1921 (1972).
8. W. Hess, *Rheol. Acta* **23**:477 (1984).
9. R. C.-Y. Ng and L. G. Leal, *Rheol. Acta* **32**:25 (1993).
10. W. W. Graessley, *Adv. Polym. Sci.* **16**:1 (1974).
11. G. S. Grest and K. Kremer, *Phys. Rev. A* **33**:3628 (1986).
12. K. Kremer, G. S. Grest, and I. Carmesin, *Phys. Rev. Lett.* **61**:566 (1988).
13. I. Bitzanis and G. Hadziioannou, *J. Chem. Phys.* **92**:3827 (1990).
14. J. W. Rudisill and P. T. Cummings, *Rheol. Acta* **30**:33 (1991).
15. B. Z. Dlugogorski, I. Grmela, and P. J. Carreau, *J. Non-Newt. Fl. Mech.* **48**:303 (1993).
16. B. Z. Dlugogorski, I. Grmela, and P. J. Carreau, *J. Non-Newt. Fl. Mech.* **49**:23 (1993).
17. D. L. Ermak and J. A. McCammon, *J. Chem. Phys.* **69**:1352 (1978).
18. F. G. Diaz, J. Garcia de la Torre, and J. J. Freire, *Polymer* **30**:259 (1989).
19. H. A. Kramers, *Physica* **11**:1 (1944).
20. A. Peterlin, *Makromol. Chem.* **44**:338 (1961).
21. A. Peterlin, *J. Chem. Phys.* **33**:1799 (1960).
22. A. J. Kishbaugh and A. J. McHugh, *J. Non-Newt. Fluid Mech.* **34**:181 (1990).